AGU PUBLICATIONS

JGR

Journal of Geophysical Research: Atmospheres

RESEARCH ARTICLE
10.1002/2016JD025904

Key Points:
- An improved quasi-stochastic model that allows a large drop to collide with a small drop more than one time in a time step is examined
- The improved model makes large drops become larger and accelerates large-drop formation by a few minutes compared to the normal model
- Using a cloud-resolving model, it is shown that the onset of surface precipitation is accelerated with the improved model

Correspondence to:
J.-J. Baik,
jjbaik@snu.ac.kr

Citation:
Lkhamjav, J., H. Lee, Y.-L. Jeon, and J.-J. Baik (2017), Examination of an improved quasi-stochastic model for the collisional growth of drops, *J. Geophys. Res. Atmos.*, *122*, 1713–1724, doi:10.1002/2016JD025904.

Received 6 SEP 2016
Accepted 17 JAN 2017
Accepted article online 20 JAN 2017
Published online 2 FEB 2017

Examination of an improved quasi-stochastic model for the collisional growth of drops

Jambajamts Lkhamjav[1], Hyunho Lee[1], Ye-Lim Jeon[1], and Jong-Jin Baik[1]

[1]School of Earth and Environmental Sciences, Seoul National University, Seoul, South Korea

Abstract The evolution of cloud drop size distribution due to the collision-coalescence process is generally described by a quasi-stochastic model that solves the stochastic collection equation in a deterministic way. In this study, an improved quasi-stochastic (IQS) model, which is derived by rigorously considering a finite model time step, is examined in the context of comparison with the normal quasi-stochastic (NQS) model. The IQS model allows a large collector drop to collide with a small collected drop more than one time in a model time step even if the collision probability is small. The number distribution of collector drops then follows the Poisson distribution with respect to the number of collisions. Using a box model that takes turbulence-induced collision enhancement into account, it is found that large drops in the IQS model tend to have larger sizes than those in the NQS model and that the IQS model accelerates large-drop formation by a few minutes compared to the NQS model. The effects of the IQS model depend on the model time step and the shape of initial drop size distribution. The IQS model is incorporated into a detailed bin microphysics scheme that is coupled with the Weather Research and Forecasting model, and a single warm cloud is simulated under idealized environmental conditions. It is found that the onset of surface precipitation is accelerated in the IQS model.

1. Introduction

Cloud drops with radii smaller than ~15 μm grow efficiently by diffusion of water vapor. However, although water vapor diffusion in a turbulent environment is somewhat controversial [*McGraw and Liu*, 2006; *Grabowski and Wang*, 2013], droplet growth by water vapor diffusion tends to be inefficient as the drop size increases, and cloud drops with radii larger than ~40 μm largely grow by collision-coalescence [*Langmuir*, 1948; *Kogan*, 1993; *Beard and Ochs*, 1993; *Pruppacher and Klett*, 1997]. Therefore, drop collision-coalescence is an important process in increasing drop size in warm clouds. Many studies on drop collision-coalescence have been performed using theoretical, experimental, and numerical approaches.

Two models have been proposed to describe the collisional growth of drops: the continuous model and the stochastic model [*Gillespie*, 1975a; *Pruppacher and Klett*, 1997]. The continuous model assumes that all drops of the same size grow by the same growth rate. The continuous model predicts very slow formation of large drops, which is mainly caused by ignoring the stochastic nature in drop collision that occurs in real clouds. *Telford* [1955] first introduced the stochastic interpretation for the modeling of drop collision, in which not all the drops grow by the same growth rate but some drops are involved in collision while others are not. *Telford* [1955] derived the stochastic model that solves the stochastic collection equation (SCE) to describe the collisional growth of drops. *Twomey* [1964] showed that the stochastic model substantially accelerates the formation of large drops compared to the continuous model.

Gillespie [1972, 1975b] and *Bayewitz et al.* [1974] considered the stochastic nature of drop collision more rigorously and showed that $N(m; t)$, which corresponds to the number of drops with mass m at time t, is replaced by $P(n, m; t)$, which corresponds to the probability that there are n drops with mass m at time t, as a predicted variable. *Gillespie* [1975a] called the newly proposed model a pure stochastic model and called the previously used stochastic model a quasi-stochastic model. *Wang et al.* [2006] further improved the pure stochastic model by specifying the range of drop size in calculating covariance to exclude unphysical coalescence and by requiring the mass conservation in solving the SCE. *Alfonso et al.* [2013] applied the turbulence-induced collision enhancement [*Pinsky et al.*, 2008] to the pure stochastic model and introduced so-called "sol-gel transition" in describing large-drop formation.

The pure stochastic model is regarded as accurately describing the evolution of drop size distribution due to collision. However, the pure stochastic model generally requires a huge amount of computing time because numerous Monte Carlo experiments have to be done to acquire reasonable statistics (mean and deviation) on

the drop size distribution. Some efforts have been made to improve the efficiency of the pure stochastic model [e.g., *Alfonso*, 2015]. Because the quasi-stochastic model has better computational efficiency compared to the pure stochastic model and higher accuracy compared to the continuous model, thus far, the quasi-stochastic model has been the most viable way to treat the collisional growth of drops in cloud models.

Gillespie [1975a] showed that if a collector drop is assumed either to collide with a collected drop or not to collide with a collected drop in an infinitesimal time interval dt, the number distribution of collector drops with respect to their masses (or equivalently to the number of collisions) is given as the Poisson distribution at any given time. Although there is no proper reason that a model time step Δt should be regarded as the same as dt, however, almost all models that adopt the quasi-stochastic model regard Δt as the same as dt in *Gillespie* [1975a] and allow a collector drop to collide with a collected drop only one time in Δt, hence neglecting the drop size distribution broadening in a model time step. *Young* [1975] first recognized the problem and introduced the Poisson distribution to represent the evolution of drop size distribution in a model time step Δt. However, *Young* [1975] considered only one case and concluded that the consideration of the Poisson distribution in a time step of 5 s accelerates the evolution of drop size distribution by only a few seconds.

In this study, the Poisson distribution in the quasi-stochastic model is revisited and examined under various initial drop size distributions. Moreover, the improved model is incorporated into a detailed bin microphysics scheme that is coupled with a cloud-resolving model and the effects of the improved model on cloud development and precipitation are investigated. The turbulence-induced collision enhancement [*Pinsky et al.*, 2008] is also taken into account to accurately describe the evolution of drop size distribution. In this study, the quasi-stochastic model with the Poisson distribution is referred to as an improved quasi-stochastic (IQS) model, while the quasi-stochastic model that allows a collector drop to collide with a collected drop only one time in a finite model time step is referred to as the normal quasi-stochastic (NQS) model.

The theoretical background of the IQS model is given in section 2. The results from a box model and a cloud-resolving model are presented and discussed in section 2. A summary and conclusions are given in section 4.

2. Theoretical Background

The basic concept of the IQS model was introduced in *Gillespie* [1975a] and *Young* [1975]. Here a rigorous derivation of the IQS model is given. The SCE, which describes the rate of change of drop number concentration due to the collection between drops, is given in an integro-differential equation form as

$$\frac{\partial f(m)}{\partial t} = \frac{1}{2}\int_0^m f\left(m'\right) f\left(m-m'\right) K\left(m', m-m'\right) dm' - \int_0^\infty f(m) f\left(m'\right) K\left(m, m'\right) dm', \tag{1}$$

where $f(m)dm$ is the drop number concentration in the mass interval of $[m, m+dm]$ and K is the collection kernel that is the product of swept volume and collection efficiency. K is given as

$$K(r_1, r_2) = \pi (r_1 + r_2)^2 |v_t(r_1) - v_t(r_2)| \eta, \tag{2}$$

where r_1 and r_2 are the radii of drops, v_t is the drop terminal velocity, and η is the collection efficiency.

If discretized grid bins are adopted to represent the drop size distribution, equation (1) can be expressed in a discretized form as [e.g., *Straka*, 2009]

$$\frac{\partial n_k}{\partial t} = \frac{1}{2}\sum_{i=1}^{k-1} n_i n_j K_{ij} - \sum_{i=1}^{N} n_k n_i K_{ki}, \tag{3}$$

where n_i, n_j, and n_k are the drop number concentrations in the ith, jth, and kth bins, respectively; K_{ij} is the collection kernel between the ith and jth bins; and N is the largest bin number. The drop masses in the ith, jth, and kth bins m_i, m_j, and m_k satisfy $m_i + m_j = m_k$. Based on equation (3), if only collision between drops in the ith and jth bins is considered, changes in number concentration in the ith, jth, and kth bins in a given model time step Δt are expressed as

$$\Delta n_k = n_i n_j K_{ij} \Delta t, \tag{4a}$$

$$\Delta n_i = \Delta n_j = -\Delta n_k. \tag{4b}$$

Equation (4b) can be expressed as

$$\Delta n_i = -p_i n_i, \tag{5a}$$

$$\Delta n_j = -p_j n_j, \tag{5b}$$

where p_i and p_j are equal to $n_j K_{ij} \Delta t$ and $n_i K_{ij} \Delta t$, respectively. Based on equations (5a) and (5b), collection between drops can be interpreted in a quasi-stochastic way as follows: if p_i is sufficiently small so that it is smaller than 1, then the collection probability for drops in the ith bin to collide with drops in the jth bin in a model time step is p_i so the number of drops that are involved in collision is $p_i n_i$ out of n_i. The same is true for drops in the jth bin.

The collection probability is expressed as the product of number concentration of collected drops, swept volume, collection efficiency, and model time step. Because the model time step used in numerical cloud models is finite, the model time step can be divided into subtime steps, which results in some collector drops that can collide with collected drops more than one time even with sufficiently small collection probability. Let the model time step Δt be divided into M subtime steps. Because the collection probability is linearly proportional to the model time step, the collection probability in the subtime step is p/M, where p is the collection probability for a given drop pair in a model time step Δt. If collision events are assumed to be independent from each other and the change in collection kernel during a model time step is negligible, then the probability of collision x times when the given model time step is divided into M subtime steps is given as

$$p_M(x) = {}_M C_x \left(\frac{p}{M}\right)^x \left(1 - \frac{p}{M}\right)^{M-x}. \tag{6}$$

Equation (6) is the binomial distribution. The number of subtime steps can be as large as infinity. Then, the final form of the probability of collision x times in the model time step is given as

$$\lim_{M\to\infty} p_M(x) = \frac{p^x e^{-p}}{x!}, \tag{7}$$

which is the Poisson distribution. Equation (7) is also found in *Young* [1975].

It is noted that the average number of collisions in the model time step in equation (7) is p, which is the same as in the NQS model. Thus, the IQS model introduced in this study (equation (7)) does not increase the average number of collisions. Rather, by rigorously considering a finite model time step, some collector drops are allowed to collide with collected drops more than one time in the model time step. In the IQS model, the probability of noncollision is increased from $1-p$ to e^{-p} and the probability of one-time collision is decreased from p to pe^{-p}. While in the NQS model the collector drop either collides one time or does not collide in the model time step, in the IQS model collisions more than one time are allowed, thus resulting in a wider size spectrum of collector drops. Therefore, the IQS model is expected to accelerate the formation of large drops by both considering some collector drops that have more chances to collide with collected drops and broadening the drop size distribution that can further accelerate collision.

It is also noted that p sometimes exceeds 1 depending on the number concentrations of drops, the size and terminal velocity of drops, and the model time step. Under this situation, the NQS model treats the collision in the same way as the continuous model; all of collector drops collide with collected drops p times. On the other hand, the IQS model treats the collision in the same way as when p is less than 1, which is another advantage of the IQS model over the NQS model. When p is sufficiently large, it is known that equation (7) is approximated by the normal distribution, which simplifies the calculation.

In this study, the turbulence-induced collision enhancement (TICE) between drops [*Pinsky et al*., 2008] is taken into account. It is known that turbulence increases the velocity difference of drops, the correlation of drop number concentrations, and the collision efficiency that is related to aerodynamic properties. *Pinsky et al*. [2008] provided TICE in a tabulated form that is a function of radii of drop pair and the turbulence intensity. Therefore, in this study, we can calculate the evolution of drop size distribution with high accuracy using the IQS model that includes the TICE.

3. Results and Discussion

3.1. Box Model

To examine the evolution of drop size distribution and the formation of large drops using the NQS and IQS models, a simple box model that considers only collision of drops is employed in this study. To calculate the collection kernel (equation (2)), the terminal velocity of drops in *Beard* [1976], the collision efficiency of drops in *Pinsky et al*. [2001], and the TICE in *Pinsky et al*. [2008] are adopted. The coalescence efficiency is assumed to be 1. The drop size distribution is represented using a bin method with 80 mass-doubling bins, in which drop masses are doubled every two bins. The SCE is solved using the mass conservative exponential flux method proposed in *Bott* [1998, 2000]. The initial drop size distribution is given as a lognormal distribution

$$F(r) = \frac{L}{\sqrt{2\pi}\sigma} \exp\left[-\frac{(\log_2 r - \log_2 r_c)^2}{2\sigma^2}\right], \tag{8}$$

where $F(r)$ is the mass concentration of drops with radii of r, L is the total liquid water content, and r_c and σ are the median and standard deviation of the distribution, respectively. L is set to 1 g m^{-3}. In the control experiments, r_c and σ are set to 10 μm and 0.33, respectively, and the time step Δt is 10 s. The model is integrated for 90 min.

Figure 1 shows the time evolution of mass-size distributions of drops obtained using the NQS and IQS models and the difference between the two models in the control experiments. Also, the mass-size distributions at $t = 30$ min are shown. In both the models, the rapid mass transition from small drops to large drops is clearly observed at t~25 min (Figures 1a and 1b). This reflects the nature of drop growth: when the size of drops is relatively small (smaller than ~15 μm), collision between drops is less active so the growth of drops is relatively slow. However, once a small number of relatively large drops (larger than ~40 μm) form, the large drops can effectively grow by collecting small drops. This characteristic is also shown in many previous studies [e.g., *Berry and Reinhardt*, 1974; *Khain et al*., 2000].

Before the appearance of large drops ($t < 25$ min), the results obtained using the NQS and IQS models are very similar to each other. The difference between the two models is observed after t~25 min, where the size of large drops tends to be increased in the IQS model (Figure 1c). This is because in the IQS model some drops have more chances to collide with other drops than those in the NQS model, which causes an increase in relatively large drops. The difference in the results is persistent until the end of the time integration. The drop size distribution at $t = 30$ min clearly shows that large drops in the IQS model tend to have larger sizes than those in the NQS model, while there is little difference in the size distribution of small drops (Figure 1d). These effects of the IQS model are also found to be similar when other initial drop size distributions, such as the gamma distribution and the Weibull distribution [*Costa et al*., 2000], are used.

Sensitivity experiments are conducted. First, experiments in which the model time step is reduced from 10 s to 1 s are conducted because it is expected that the difference between the results of the IQS and NQS models would increase with increased model time step. Figure 2 shows the results with $\Delta t = 1$ s. Figures 2a and 2b are similar to Figures 1a and 1b, respectively, which indicates that both the models show reasonable drop size distribution evolution with Δt~10 s. This agrees with the result in *Bott* [2000]. The difference between the model results with $\Delta t = 1$ s is depicted in Figure 2c, in which there is still difference between the model results even with the small model time step. The difference also persists until the end of the time integration. Compared to Figure 1c, Figure 2c clearly shows that the difference is reduced with the small model time step, as expected. Compared to Figure 1d, Figure 2d also shows that the difference in the shift of the size distribution of large drops is reduced.

Sensitivity experiments with different drop size distribution parameters are also conducted. Figures 3a–3c and 3d–3f are the same as Figures 1a–1c but with $r_c = 8$ μm and 12 μm, respectively. Corresponding initial drop number concentrations are 761 and 226 cm^{-3}, respectively. For $r_c = 8$ μm, the formation of large drops are substantially delayed in both the NQS and IQS models compared to the control experiments. The rapid mass transition from small drops to large drops occurs at t~40 min, while it occurs at t~25 min in the control experiments. The difference in the size distribution of large drops obtained using the two models is larger than that in the control experiments (Figure 3c compared to Figure 1c).

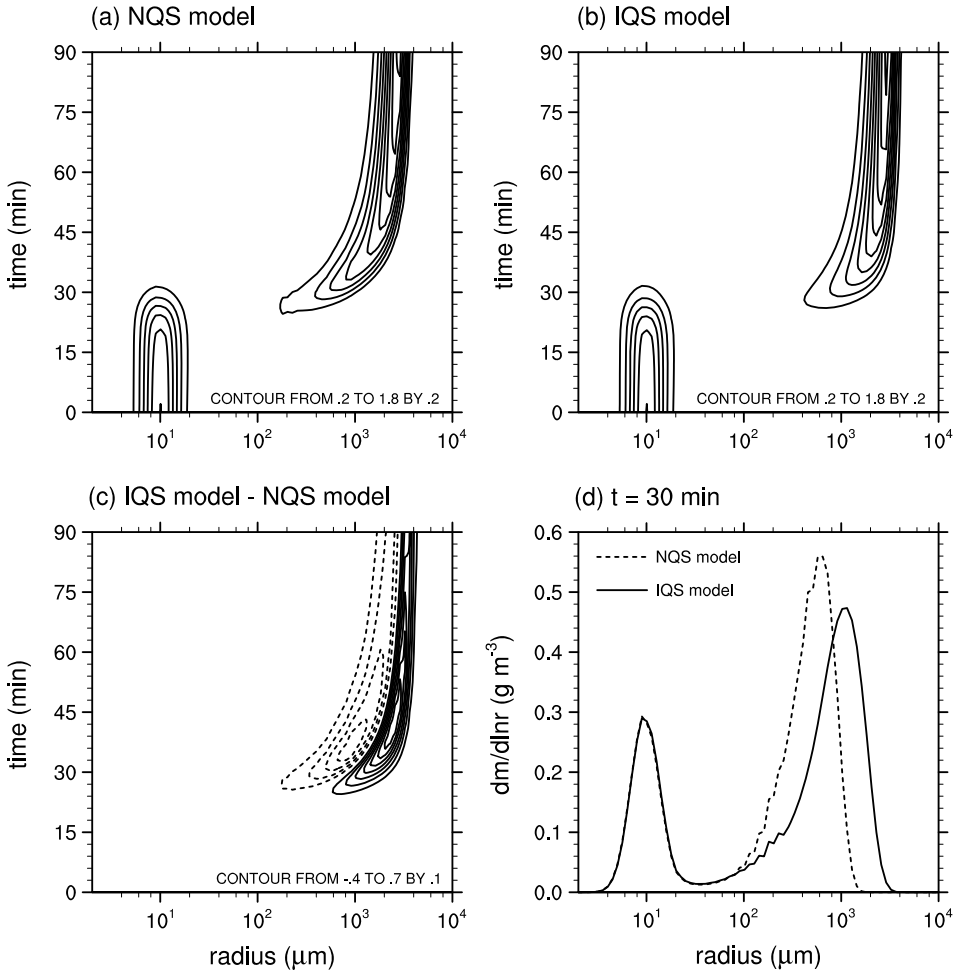

Figure 1. Time evolution of mass-size distributions of drops (g m^{-3}) obtained using (a) the NQS model, (b) the IQS model, and (c) difference between the two models in the control experiments. In Figure 1c, positive and negative values are depicted by solid and dashed lines, respectively. (d) Mass-size distributions of drops obtained using the NQS and IQS models at $t = 30$ min.

Figures 3d–3f show the results for $r_c = 12$ μm. The formation of large drops and the mass transition from small drops to large drops are considerably accelerated compared to the control experiments. The rapid mass transition from small drops to large drops is observed at t~18 min. The difference in the size distribution of large drops obtained using the two models is smaller than that in the control experiments (Figure 3f compared to Figure 1c).

Figures 3g–3i and 3j–3l show the results for $\sigma = 0.22$ and 0.44, respectively. Because σ is the standard deviation of the initial drop size distribution that is given in a lognormal distribution, a larger σ indicates a more dispersed initial drop size distribution. Differences between the two models when the initial dispersion is relatively small are similar to those when the initial median drop size is relatively small (Figures 3c and 3i), and differences between the two models when the initial dispersion is relatively large are similar to those when the initial median drop size is relatively large (Figures 3f and 3l). The effect of the IQS model on the size distribution of large drops is larger in an environment in which the large-drop formation is less favorable, which includes either smaller initial median drop size or smaller initial drop size dispersion.

Figure 4 shows the time series of the total mass of large drops in the control experiments and the other sensitivity experiments. In this figure, a large drop is defined using a critical radius of 1 mm. In all experiments, the IQS model accelerates large-drop formation. Therefore, the IQS model affects not only the size distribution of large drops but also the time required for large-drop formation. In contrast to the size distribution of large drops, however, the difference in the time required for large-drop formation is larger when the

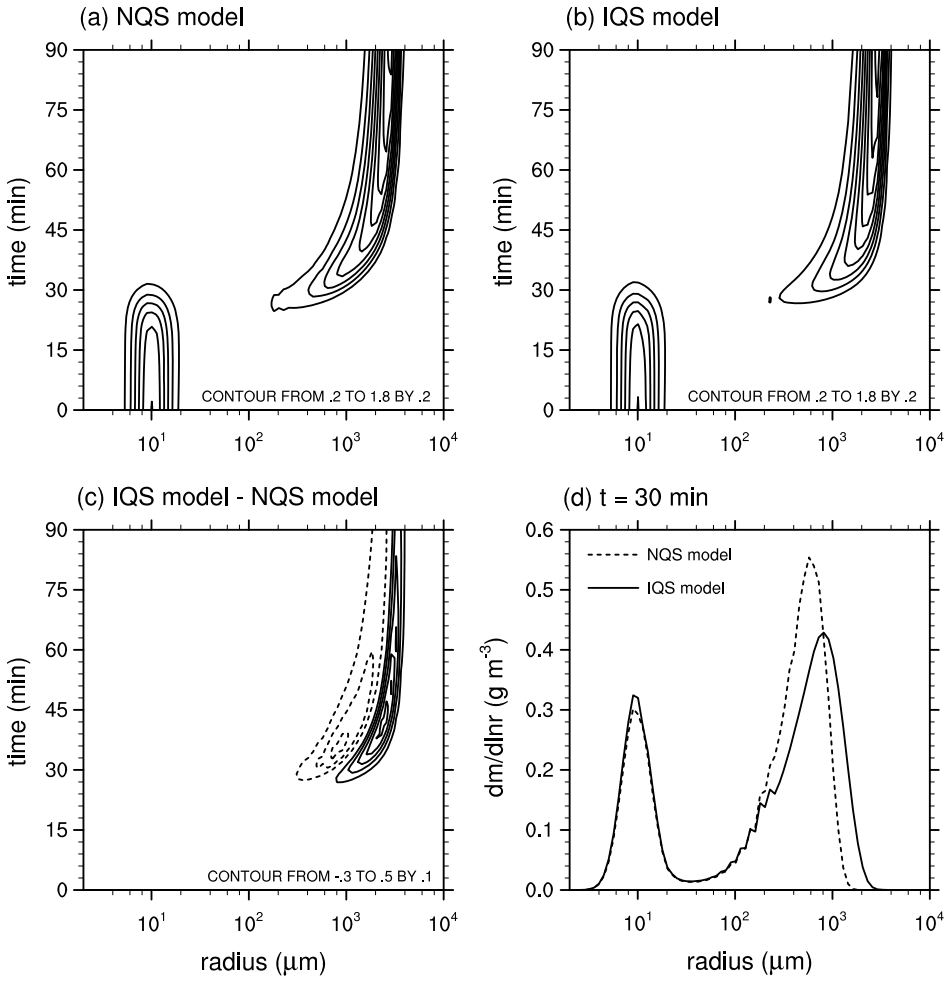

Figure 2. (a–d) Same as in Figure 1 but for $\Delta t = 1$ s.

large-drop formation is more favorable (larger r_c or larger σ) than when the large-drop formation is less favorable (smaller r_c or smaller σ).

It is known that an increase in aerosol number concentration induces a decrease in mean drop size at the early cloud development stage, hence causing a delay in large-drop formation [e.g., *Albrecht*, 1989; *Rosenfeld*, 1999; *Choi et al.*, 2014]. In this study, it is shown that the difference in the time required for large-drop formation caused by different initial median drop sizes and different initial dispersion parameters of drop size distribution is larger in the IQS model than in the NQS model. Therefore, it might be deduced that the IQS model somewhat amplifies the aerosol effect that is known to delay large-drop formation. However, because the aerosol effect related to the large-drop formation is very complex in nature depending on various environmental conditions, careful approaches and in-depth studies are needed. The difference is larger with a larger model time step, as expected.

The difference in the time of large-drop formation between the NQS and IQS models in this study is approximately a few minutes, from 1–2 min to ~5 min, which is much larger than a few seconds that is reported in *Young* [1975]. The difference depends on the initial drop size distribution and the model time step.

3.2. Cloud-Resolving Model

To examine the effects on cloud development and precipitation, the IQS model is implemented into a microphysics scheme, which is in Hebrew University Cloud Model (HUCM) that originally adopts the NQS model to solve the SCE. The microphysics scheme in HUCM uses a bin method; it represents each hydrometeor size distribution at each grid point and at each time instance using 43 mass-doubling bins. A detailed

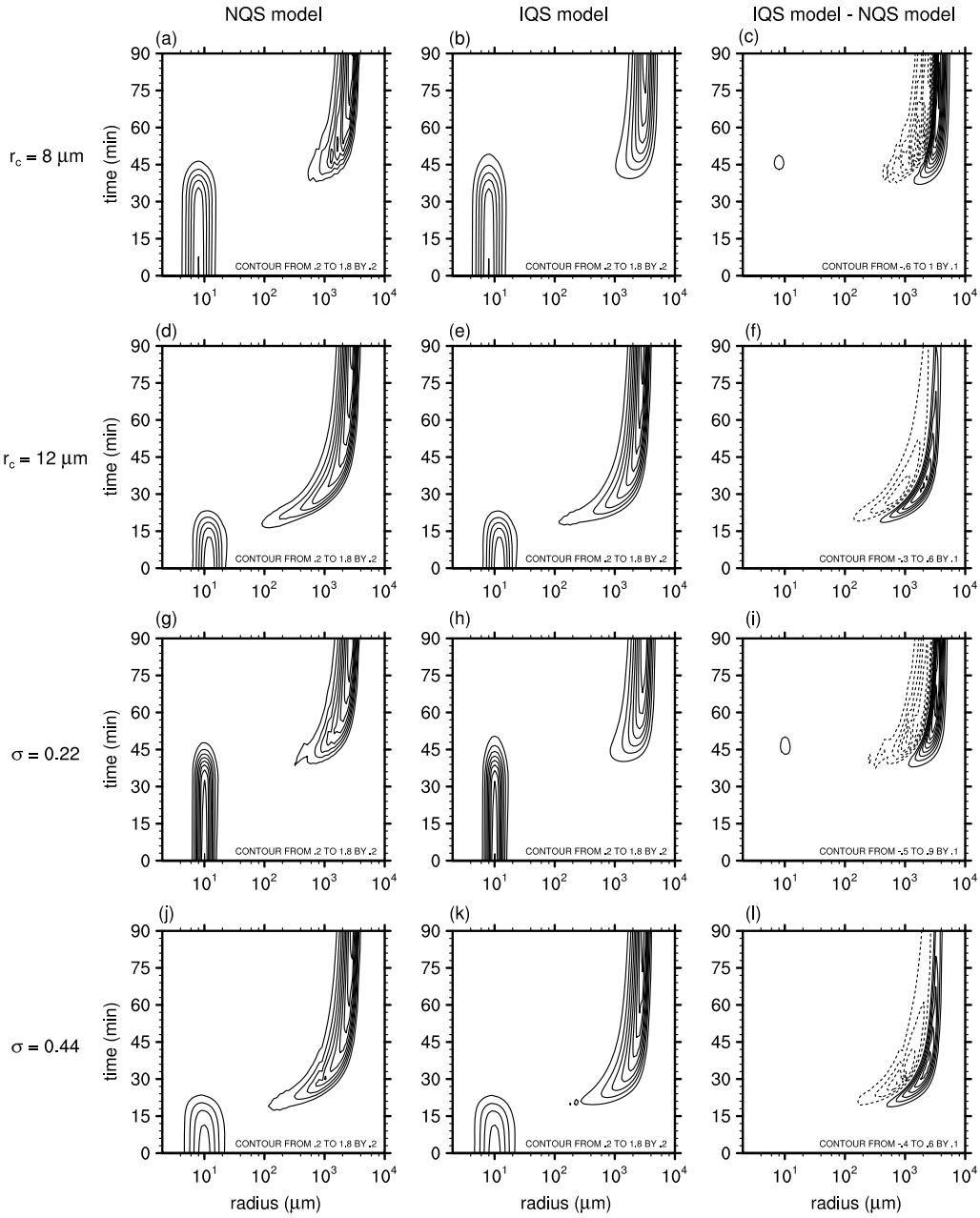

Figure 3. Same as in Figures 1a–1c but for the sensitivity experiments with varied r_C and σ. (a–c) The experiments with $r_C = 8$ μm, (d–f) the experiments with $r_C = 12$ μm, (g–i) the experiments with $\sigma = 0.22$, and (j–l) the experiments with $\sigma = 0.44$.

description of the microphysics scheme in HUCM is given in *Khain et al*. [2011]. TICE proposed in *Pinsky et al*. [2008] that is considered in the box model is also taken into account in the microphysics scheme in HUCM.

The Weather Research and Forecasting (WRF) model version 3.6.1 [*Skamarock et al*., 2008] coupled with the microphysics scheme in HUCM [*Lee and Baik*, 2016] is used in this study. Numerical experiments that simulate a 2-D single warm cloud are conducted using the WRF model. The experimental setup is established following *Lee et al*. [2015]. The thermodynamic sounding used by *Ogura and Takahashi* [1973], which is characterized by a warm and humid environment and a strong capping inversion layer near $z = 3$ km, is adopted for simulations. The initial aerosol number concentration near the surface is set to 300 cm^{-3}. The model domain size is 51.2 km in the horizontal direction and 8 km in the vertical direction. The grid spacing is 50 m in both the horizontal and vertical directions. The model is integrated for 60 min with a time step of 1 s.

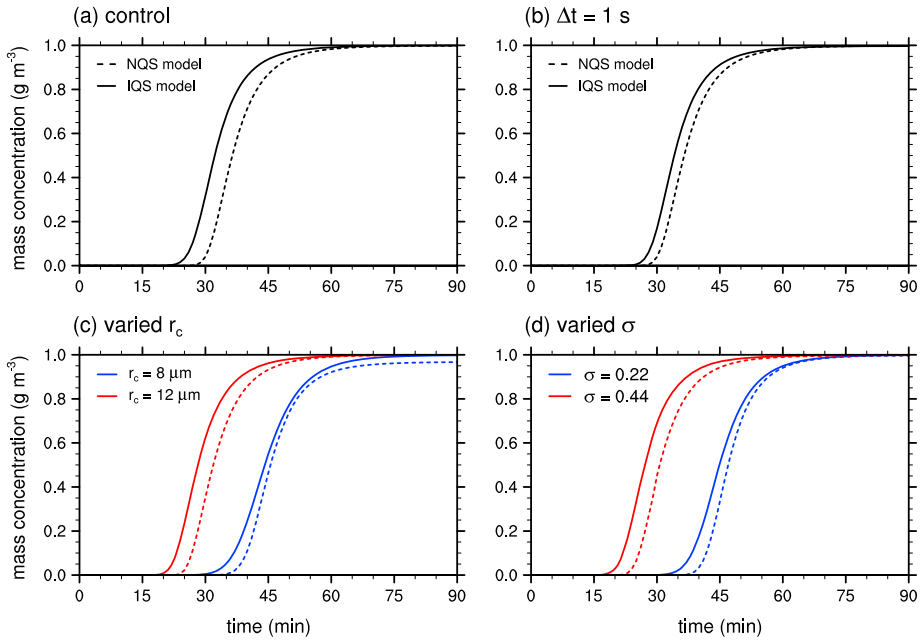

Figure 4. Time series of the total mass concentration of large drops ($r > 1$ mm) in (a) the control experiments, (b) the sensitivity experiments with $\Delta t = 1$ s, (c) the sensitivity experiments with $r_c = 8$ and 12 μm, and (d) the sensitivity experiments with $\sigma = 0.22$ and 0.44. In Figures 4c and 4d, the dashed lines are the results of the NQS model and the solid lines are the results of the IQS model.

The time series of the surface precipitation rate averaged over the mostly cloudy area ($x = 13$–23 km in the model domain) in the NQS and IQS models are shown in Figure 5. While the overall precipitation patterns before t~45 min are similar to each other, the surface precipitation starts earlier in the IQS model than in the NQS model by 1–2 min, which agrees with the box model results in section 3.1. This study demonstrates that the rigorous consideration of the finite model time step can affect not only the evolution of drop size distribution in the simple box model but also cloud development and precipitation in the complex cloud-resolving model. The time series of the surface precipitation rate in the two models exhibit a large difference after t~45 min. As the first formed cloud is decaying, many small clouds form. Because they are largely affected by perturbed environmental conditions, it is difficult to argue that the difference after t~45 min is caused by the IQS model, and a direct comparison between the results obtained using the two models after t~45 min is not straightforward.

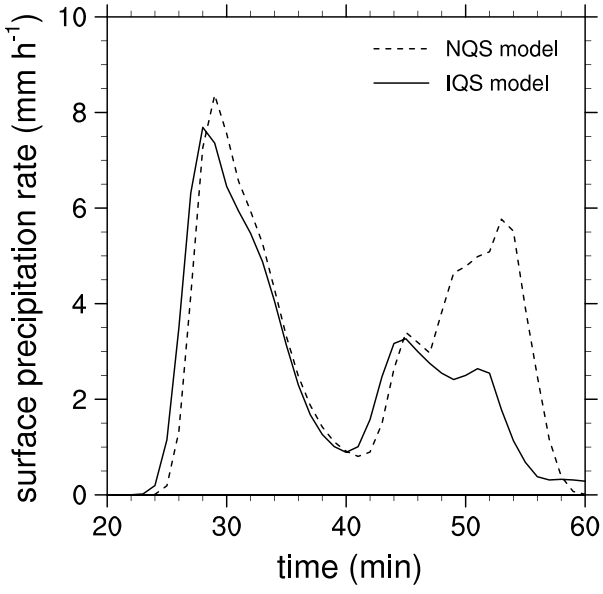

Figure 5. Time series of the surface precipitation rate averaged over $x = 13$–23 km in the NQS and IQS models.

The spatial distributions of cloud water content (CWC) and rainwater content (RWC) are examined to investigate the effects of the IQS model on cloud development and precipitation. Figure 6 shows the CWC and RWC fields and the vertical profiles of horizontally averaged CWC and RWC at $t = 23$ min. The difference in

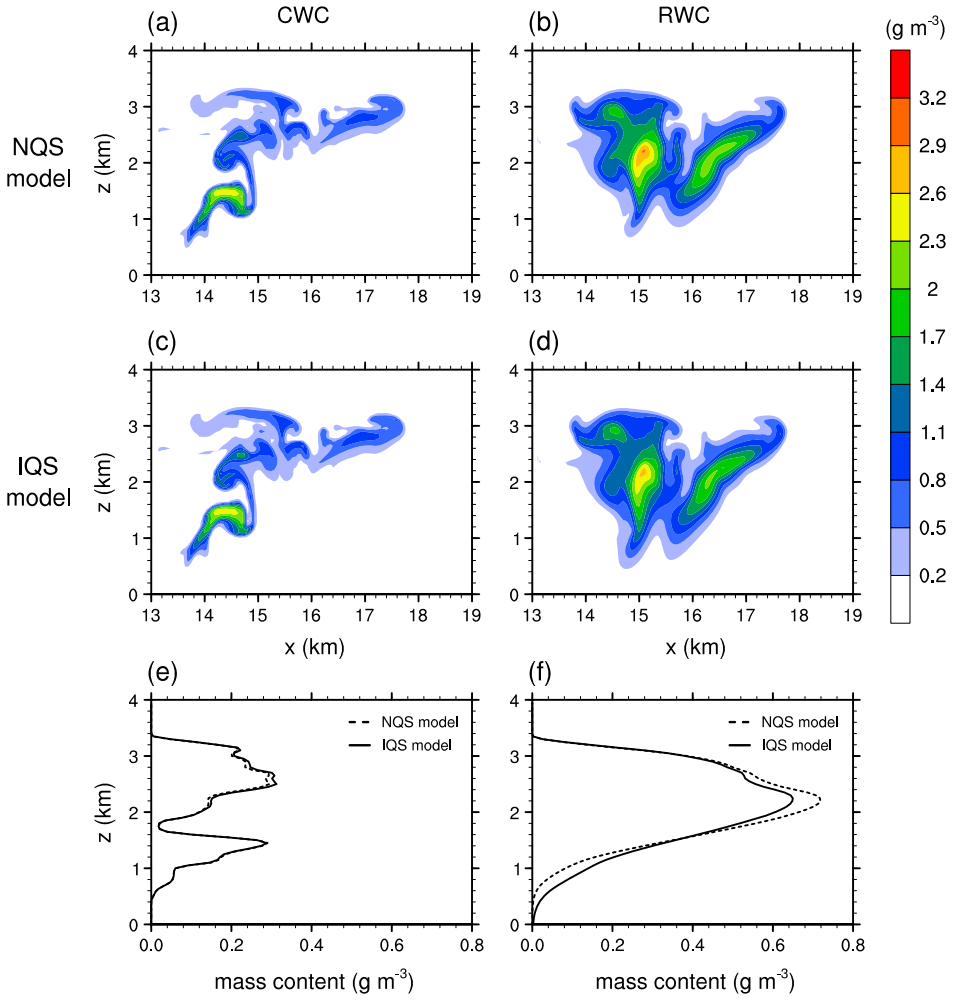

Figure 6. Fields of (a) cloud water content (CWC) and (b) rainwater content (RWC) at $t = 23$ min obtained using the NQS model. (c and d) Same as in Figures 6a and 6b, respectively, but for the IQS model. Vertical profiles of (e) CWC and (f) RWC averaged over $x = 13$–19 km at $t = 23$ min in the NQS and IQS models.

CWC between the two models is negligible (Figures 6a, 6c, and 6e) at this time, but the difference in RWC is observed (Figures 6b, 6d, and 6f). RWC in the layer $z < 1.5$ km is larger in the IQS model than in the NQS model. The IQS model accelerates large-drop formation as shown in the box model results. The large drops that form earlier fall to the lower layer earlier, so RWC in the lower layer is larger in the IQS model than in the NQS model. Over time, the difference in CWC is still very small but the difference in RWC becomes clearer (see Figure 7). At $t = 26$ min (Figure 7), when the early surface precipitation rate is rapidly increasing, RWC in the layer $z < 0.5$ km is larger in the IQS model than in the NQS model, which results in the increased early surface precipitation amount in the IQS model. It is noted that RWC in the layer $z = 0.5$–2.5 km is smaller in the IQS model than in the NQS model mainly because of the early sedimentation of larger drops in the IQS model.

Figure 8 shows the drop size distributions averaged in the area where $z < 0.5$ km and the rainwater mixing ratio is larger than 0.5 g kg^{-1} at $t = 27$ min in the NQS and IQS models. A wider spectrum of the number-size distribution of drops is seen in the IQS model (Figure 8a), which results from the Poisson distribution. The mass-size distributions of drops show that the large drops in the IQS model tend to have larger sizes than those in the NQS model, which is similar to the result of the box model (Figures 1d and 2d).

4. Summary and Conclusions

In this study, the IQS model, which is derived by rigorously considering a finite model time step for solving SCE, was examined and compared with the NQS model. In the IQS model, the probability that a large

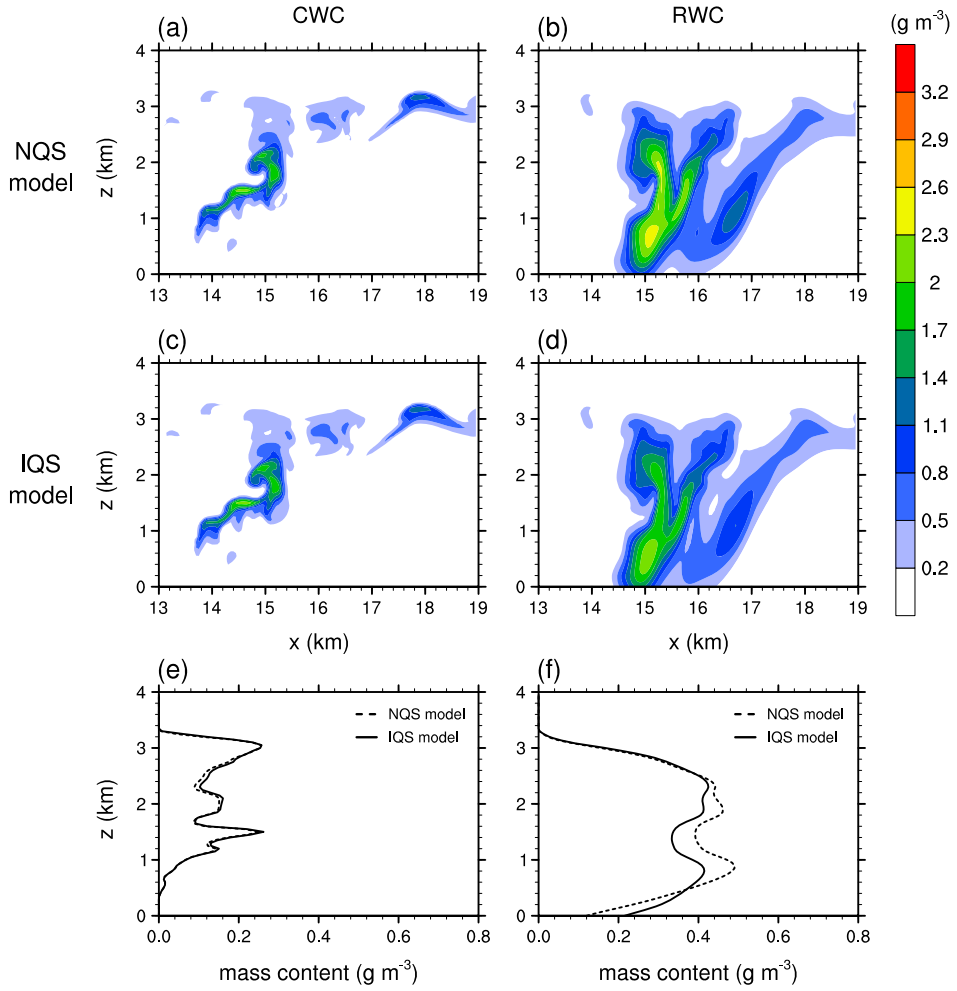

Figure 7. (a–f) Same as in Figure 6 but at $t = 26$ min.

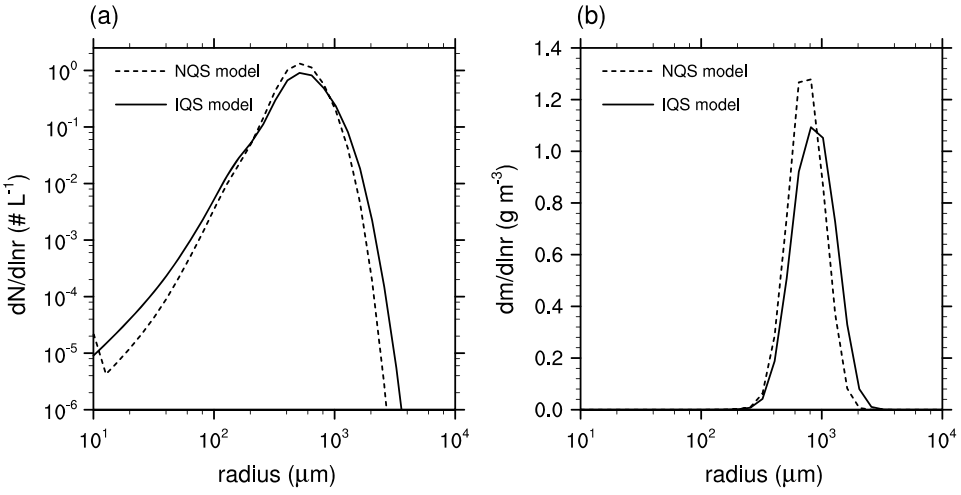

Figure 8. (a) The number- and (b) mass-size distributions of drops averaged over the area where $z < 0.5$ km and the rainwater mixing ratio ≥ 0.5 g kg^{-1} at $t = 27$ min in the NQS and IQS models.

collector drop collides with a small collected drop follows the Poisson distribution with respect to the number of collisions.

Using a box model that takes TICE into account, it was shown that the IQS model tends to increase the sizes of large drops and accelerates the large-drop formation compared to the NQS model. This is because some large collector drops are allowed to have more chances to collide with small collected drops in the IQS model. The size distribution of large drops becomes wider, which also enhances collisions. Our box model results suggest that the IQS model can partially explain the drop growth across the so-called size gap, typically referring to a radius range between ~15 and ~40 μm [*Beard and Ochs*, 1993; *Grabowski and Wang*, 2013]. The effects of the IQS model depend on the model time step and the shape of initial drop size distribution. Because the IQS model considers collision of drops in the model time step, the effects are smaller when the model time step is smaller. The shift in the size distribution of large drops is larger when the collisional growth of drops is less favorable, but the acceleration of larger-drop formation is larger when the collisional growth of drops is more favorable. The accelerated large-drop formation by the IQS model that is larger in the situation in which the collisional growth of drops is more favorable implies that the aerosol effect that is known to delay the large-drop formation could be somewhat increased in the IQS model. The acceleration of the drop size distribution evolution caused by the IQS model is a few minutes, which is much larger than that reported in *Young* [1975]. The IQS model was incorporated into a cloud-resolving model that uses a detailed bin microphysics scheme, and a single warm cloud was simulated. It was shown that the onset of surface precipitation is accelerated in the IQS model, which agrees with the box model result.

It would be interesting to investigate the effects of the IQS model on mixed-phase cloud development and precipitation under idealized environmental conditions. In real environments, the effects of the IQS model on clouds and precipitation could be very complex, but positive impacts on precipitation prediction are expected. This deserves an in-depth investigation through the simulations of many real cases.

Appendix A: The Detailed Algorithm of the IQS Model

In this appendix, the detailed algorithm of the IQS model is presented in a pseudocode form as follows:

for $i = 1, 2, 3, \ldots, N$ **do**
for $j = 1, 2, 3, \ldots, i$ **do**
  $p \leftarrow n_j \times K_{ij} \times \Delta t$
  $x \leftarrow 0$
  $p(x) \leftarrow e^{-p}$
  $S_p \leftarrow p(x)$
  loop
    $x \leftarrow x + 1$
    $p(x) \leftarrow p(x) \times p/x$
    $\Delta n_i \leftarrow n_i \times p(x)$
    $n_j \leftarrow n_j - x \times \Delta n_i$
    $S_p \leftarrow S_p + p(x)$
    $m(x) \leftarrow m_i + x \times m_j$
    $M(x) \leftarrow m(x) \times \Delta n_i$
    if $n_j \leq 0$ **or** $S_p > 1 - \varepsilon$, **then**
      break out of loop
    end if
  end loop
  $n_i \leftarrow n_i \times \{S_p - p(0)\}$
  redistribute $M(x)$
end for
end for

Here ε is a sufficiently small positive number, which is set to 10^{-5} in this study. All the other notations have the same meanings as in section 2. A simple algorithm to prevent n_j from being negative is applied. For the redistribution of $M(x)$, the method proposed in *Bott* [1998, 2000] is used, as for the NQS model.

Acknowledgments

The authors are grateful to three anonymous reviewers for providing valuable comments on this study. All data of this study are accessible via personal communication with the corresponding author (jjbaik@snu.ac.kr). The authors were supported by the Korea Meteorological Administration Research and Development Program under grant KMIPA 2015-5100. The first author was also supported by the SNU President Fellowship.

References

Albrecht, B. A. (1989), Aerosols, cloud microphysics, and fractional cloudiness, *Science*, *245*, 1227–1230.

Alfonso, L. (2015), An algorithm for the numerical solution of the multivariate master equation for stochastic coalescence, *Atmos. Chem. Phys.*, *15*, 12,315–12,326.

Alfonso, L., G. B. Raga, and D. Baumgardner (2013), The validity of the kinetic collection equation revisited—Part 3: Sol–gel transition under turbulent conditions, *Atmos. Chem. Phys.*, *13*, 521–529.

Bayewitz, M. H., J. Yerushalmi, S. Katz, and R. Shinnar (1974), The extent of correlations in a stochastic coalescence process, *J. Atmos. Sci.*, *31*, 1604–1614.

Beard, K. V. (1976), Terminal velocity and shape of cloud and precipitation drops aloft, *J. Atmos. Sci.*, *33*, 851–864.

Beard, K. V., and H. T. Ochs (1993), Warm-rain initiation: An overview of microphysical mechanisms, *J. Appl. Meteorol.*, *32*, 608–625.

Berry, E. X., and R. L. Reinhardt (1974), An analysis of cloud drop growth by collection: Part II. Single initial distributions, *J. Atmos. Sci.*, *31*, 1825–1831.

Bott, A. (1998), A flux method for the numerical solution of the stochastic collection equation, *J. Atmos. Sci.*, *55*, 2284–2293.

Bott, A. (2000), A flux method for the numerical solution of the stochastic collection equation: Extension to two-dimensional particle distribution, *J. Atmos. Sci.*, *57*, 284–294.

Choi, I.-J., T. Iguchi, S.-W. Kim, T. Nakajima, and S.-C. Yoon (2014), The effect of aerosol representation on cloud microphysical properties in Northeast Asia, *Meteorol. Atmos. Phys.*, *123*, 181–194.

Costa, A. A., C. J. Oliveira, J. C. P. Oliveira, and A. J. C. Sampaio (2000), Microphysical observations of warm cumulus clouds in Ceará, Brazil, *Atmos. Res.*, *54*, 167–199.

Gillespie, D. T. (1972), The stochastic coalescence model for cloud droplet growth, *J. Atmos. Sci.*, *29*, 1496–1510.

Gillespie, D. T. (1975a), Three models for the coalescence growth of cloud drops, *J. Atmos. Sci.*, *32*, 600–607.

Gillespie, D. T. (1975b), An exact method for numerically simulating the stochastic coalescence process in a cloud, *J. Atmos. Sci.*, *32*, 1977–1989.

Grabowski, W. W., and L.-P. Wang (2013), Growth of cloud droplets in a turbulent environment, *Annu. Rev. Fluid Mech.*, *45*, 293–324.

Khain, A., M. Ovtchinnikov, M. Pinsky, A. Pokrovsky, and H. Krugliak (2000), Notes on the state-of-the-art numerical modeling of cloud microphysics, *Atmos. Res.*, *55*, 159–224.

Khain, A., D. Rosenfeld, A. Pokrovsky, U. Blahak, and A. Ryzhkov (2011), The role of CCN in precipitation and hail in a mid-latitude storm as seen in simulations using a spectral (bin) microphysics model in a 2D dynamic frame, *Atmos. Res.*, *99*, 129–146.

Kogan, Y. L. (1993), Drop size separation in numerically simulated convective clouds and its effect on warm rain formation, *J. Atmos. Sci.*, *50*, 1238–1253.

Langmuir, I. (1948), The production of rain by a chain reaction in cumulus clouds at temperatures above freezing, *J. Meteorol.*, *5*, 175–192.

Lee, H., and J.-J. Baik (2016), Effects of turbulence-induced collision enhancement on heavy precipitation: The 21 September 2010 case over the Korean Peninsula, *J. Geophys. Res. Atmos.*, *121*, 12,319–12,342, doi:10.1002/2016JD025168.

Lee, H., J.-J. Baik, and J.-Y. Han (2015), Effects of turbulence on warm clouds and precipitation with various aerosol concentrations, *Atmos. Res.*, *153*, 19–33.

McGraw, R., and Y. Liu (2006), Brownian drift-diffusion model for evolution of droplet size distributions in turbulent clouds, *Geophys. Res. Lett.*, *33*, L03802, doi:10.1029/2005GL023545.

Ogura, Y., and T. Takahashi (1973), The development of warm rain in a cumulus cloud, *J. Atmos. Sci.*, *30*, 262–277.

Pinsky, M., A. Khain, and M. Shapiro (2001), Collision efficiency of drops in a wide range of Reynolds numbers: Effects of pressure on spectrum evolution, *J. Atmos. Sci.*, *58*, 742–764.

Pinsky, M., A. Khain, and H. Krugliak (2008), Collisions of cloud droplets in a turbulent flow. Part V: Application of detailed tables of turbulent collision rate enhancement to simulation of droplet spectra evolution, *J. Atmos. Sci.*, *65*, 357–374.

Pruppacher, H. R., and J. D. Klett (1997), *Microphysics of Clouds and Precipitation*, Kluwer Acad., Netherlands.

Rosenfeld, D. (1999), TRMM observed first direct evidence of smoke from forest fires inhibiting rainfall, *Geophys. Res. Lett.*, *26*, 3105–3108, doi:10.1029/1999GL006066.

Skamarock, W. C., J. B. Klemp, J. Dudhia, D. O. Gill, D. M. Barker, M. G. Duda, X.-Y. Huang, W. Wang, and J. G. Powers (2008), A description of the advanced research WRF version 3, *NCAR Tech. Note NCAR/TN-475 + STR*, NCAR, Boulder, Colo.

Straka, J. M. (2009), *Cloud and Precipitation Microphysics: Principles and Parameterizations*, Cambridge Univ. Press, U. K.

Telford, J. W. (1955), A new aspect of coalescence theory, *J. Meteorol.*, *12*, 436–444.

Twomey, S. (1964), Statistical effects in the evolution of a distribution of cloud droplets by coalescence, *J. Atmos. Sci.*, *21*, 553–557.

Wang, L. P., Y. Xue, O. Ayala, and W. W. Grabowski (2006), Effect of stochastic coalescence and air turbulence on the size distribution of cloud droplets, *Atmos. Res.*, *82*, 416–432.

Young, K. C. (1975), The evolution of drop spectra due to condensation, coalescence and breakup, *J. Atmos. Sci.*, *32*, 965–973.